International Journal of ChemTech Research
CODEN (USA): IJCRGG, ISSN: 0974-4290, ISSN(Online):2455-9555
Vol.12 No.02, pp 299-309, 2019

Structural, Dielectric and magneto-electric properties of La and Co Co-Substituted $BiFeO_3$ Ceramics

Senbeto Kena Etana*, P.Vijarya Bhaskar Rao

Department of Physics, Wollega University, Ethiopia

Abstract : $Bi_{1-x}La_xFe_{0.85}Co_{0.15}O_3$(x = 0.1,0.15)Ceramics have been prepared by sol-gel technique. X-ray diffraction data indicated a phase transition from rhombohedra with space group R3c toorthorhombic structure and decreasing in crystallite size from26.27nm to 21.05nm for x=0.1, 0.15, respectively. The activation energy for electrical conduction has been calculated from the Arrhenius plot using impedance measurement. The activation energy for the grain conduction was found to be increased from 0.286 eV to 0.38eV for x=0.1, 0.15, respectively measured in the temperature ranges ($300^oC, 350^oC, 400^oC, 450^o, 500^oC$). The vibrating sample magnetometer (VSM)results showed that the saturation magnetization (Ms) increased from 13.24emu/g for x=0.1 to 39.59 emu/g for x=0.15, due to the collapse of spin cycloid structure. The remnant magnetization (Mr) is also correspondingly enhanced from 3.43 emu/g to 11.88emu/g.

Keywords : nano-particle, multi-ferroics, dielectric constant, dielectric loss, bismuth ferrites, magnetization.

1. Introduction

Multiferroic materials exhibiting coexistence and simultaneous coupling of ferroelectricity and ferromagnetism have recently attracted considerable attention due to their potential applications and attractive physical phenomena[1,2].As one of representative single-phase multi-ferroics, BiFeO3 (BFO) is known to be the only material that is both ferroelectric (T_C~830^{o}C) and anti-ferromagnetic (T_N ~ 370^{o}C) at room temperature, which makes it an excellent possible candidate for practical application[3,4].However, synthesis of a BFO single-phase material is slightly complicated due to some reasons: (i) large leakage current in BFO ceramics is induced by impurities; (ii) non-stoichiometry and oxygen vacancies, which made the material to be difficult to achieve good ferroelectric properties. So the chemical modification by co-substitution of rare-earth or transition metal ions into the BFO crystal was proposed[5,6]. Previous studies showed that the enhancement of magnetic properties of BFO material was obtained due to Bi-sites replaced by rare-earth or Fe-sites replaced by transition metal ions[7-9]. The substitution of rare- earthions at the Bi-sites is also effective way to decrease leakage current, to enhance ferromagnetic, meanwhile the substitution of transition metalions at the Fe-sites contributes to improving ferroelectric properties[10].

DOI= http://dx.doi.org/10.20902/IJCTR.2019.120239

Zhao and Yun, (2013) investigated the impacts of simultaneously co doping of Ho and Mn in $BiFeO_3$nano-particles and enhanced ferromagnetism was attributed due to the structural distortion and reform of the anti-parallel spin structure by Mn substitution[11]. BFO ceramics co doped with Ho and Ni cations ($Bi_{1-x}Ho_xFe_{1-y}Ni_yO_3$) by Tadic et al. (2014) using the solid-state method[12]. The investigators concluded that Ni improved ferromagnetic properties while Ho canted the magnetic exchange.

In W. Mao et al.(2014), $Bi_{0.95}Ln_{0.05}Fe_{0.95}Co_{0.05}O_3$ ceramics were synthesized, which the co doped with cobalt and rare earth metals lanthanum or Praseodymium (Ln = La, Pr) by sol–gel method. The impacts on various parameters were investigated and it was reported that the impurity phases were effectively suppressed and the magnetic properties of the two co-doped samples were significantly enhanced [13]. It was also observed from Raman results that La and Co co-doping originate a significant distortion of Fe–O bonds which may enhance magnetization and ferroelectric properties in La and Co into BFO.

Therefore, rare- earthandtransition metalco-doped $BiFeO_3$ materials are expected to enhance both ferroelectric and ferromagnetic properties for practical applications [5, 14, and 15].

In this study, we reported the synthesis of (La, Co) co-doped $BiFeO_3$ materials with different doping contents using a sol-gel technique. The Structural, dielectric and magneto-electric properties of $Bi_{1-x}La_xFe_{0.85}Co_{0.15}O_3$ (*x= 0.10, 0.15)* ceramics were investigated by their respective characterization techniques.

2. Experimental details

The $Bi_{1-x}La_xFe_{0.85}Co_{0.15}O_3$ ($x = 0.10.0.15$) ceramics were prepared using sol-gel technique.Nitrates of$(NO_3)_3.5H_2O$,$Co(NO_3)_2.6H_2O$,$Fe(NO_3)_3.9H_2O$,$La(NO_3)_3.5H_2O$ with purities more than 99.5%, were used as precursors. Citric acid ($C_6H_8O_7$) was used as chelating agent. Stoichiometric amounts of nitrates were added to doubly de-ionized water separately and mixed with citric acid in a glass beaker at room temperature, so that one mole of metal nitrates is equal to one mole of citric acid to facilitate the reaction rate. The mixed chemicals were stirredexothermally by magnetic stirrer with high velocity until uniform solution was formed. Further, the solution in beaker was placed on hot plate having magnetic stirrer and heated up to a temperature of 90^{o}C for 2hrs.

Ammonia solution (NH_3) was slowly added to the solution to control the PH value around neutral value with continuous stirring. This was continued until the solution is turned to gel. The gel has taken out on evaporating dish and was placed in hot oven at temperature 120^{0}C for four hours to become dry gel. Then, water evaporation is held by raising the temperature of the dried gel to 220^{0}C. Then the dried gel was grinded by agate mortar. The obtained powders were placed in hotfurnace and pre-sintered to 650^{o}C for 3hrs in order to remove excess hydrocarbon and some impurities. The powders were again grinded very finely and pressed to the pellet of about 1mm thick and 10mm diameter disks with hydraulic press of 12.5 ton. Finally the pellets were sintered at 850^{o}C for 3 hrs resulting in good densification. Both sides of the surface of the pellets were silvered using silver paste and heated at 100^{o}C for 1hr, for electrical measurements.

The samples phase identifications were characterized by x-ray diffraction (XRD) in the range of 2θ from 20^o to 70^o, step of 0.02^o with continuous scan rate of 0.2^o per second using *XRDML with Cu-Kαradiation(λ=1.54056$\acute{A}$), the Fourier transform infrared (FTIR) spectroscopy was used to determine the range of absorption band for further phase identification in supporting XRD.The samples surface morphologies and chemical compositions, respectively were characterized by scanning electron microscopy (SEM) and energy dispersive X-ray (EDX). The impedances were measured using impedance analyzer (Wayne Kerr). Magnetic measurement at room temperature was conducted using vibrating sample magnetometer (VSM, Lakeshore 7407 series).

3. Results and Discussion

3.1. Structural analysis

Figures 1a&b have shown the XRD patterns of $Bi_{1-x}La_xFe_{0.85}Co_{0.15}O_3$ (x=0.1, 0.15) ceramicssintered at 850^{o}C. The room temperature XRD pattern confirms the formation of crystalline single phase orthorhombic

structure with small peaks (*) associated with $Bi_{25}FeO_{40}$ impurity phase (ICDD 57594-58-8). The presence of small amount of other impurity phase cannot be ruled out during synthesis of these nano-particles.

The full width at half maximum intensity (FWHM),β of (110) and (104) main diffraction peak was utilizedto calculate the average crystallite size (D) for each sample using Debye-Scherer formula[16].

$$D = \frac{k\lambda}{\beta Cos\theta} (1)$$

Where k is the dimensionless constant with typical value of ~0.9, λ is the wavelength of Cu-kα radiation with value of 1.5418$\dot{A}$ and θ is the Bragg angle of the main peak (110)/(104).

To investigate the change in crystal structure and parameters, Rietveld refinement of the synthesized was carried out using FULLPROF suit program. The Miller indices are compared with JCPDs card no. 34-0411 and indexed as shown in the figures 1. The refined structural parameters of the samples are enlisted in Table 1.

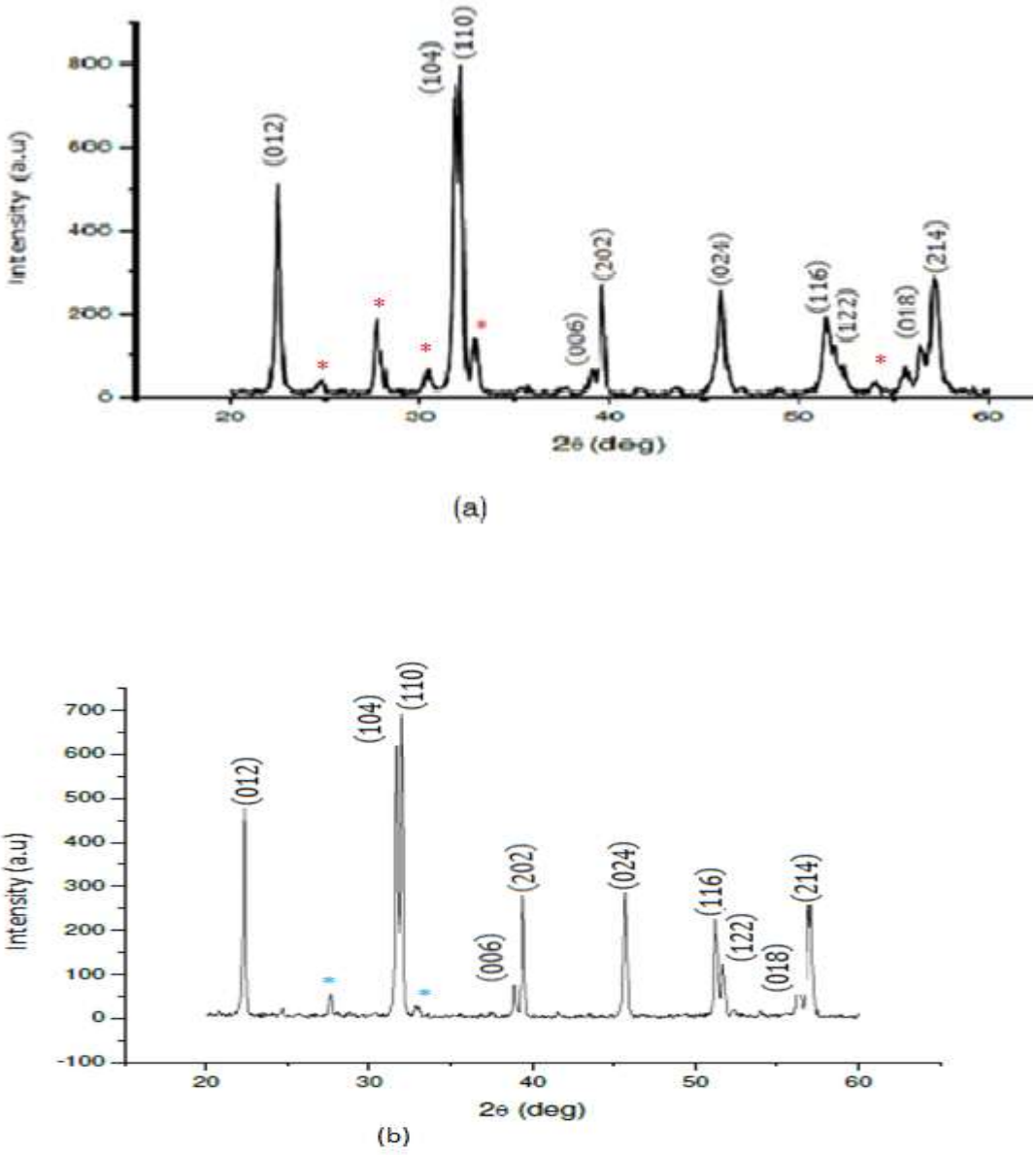

Figure 1 XRD spectra of $Bi_{1-x}La_xFe_{0.85}Co_{0.15}O_3$ for a) x=0.1 b) x=0.15

The doping concentrations from x=0.1 to x=0.15 have shown improved crystallite structure by disappearing extra peaks as compared to un-doped BFO [17,18]

Table 1The structural parameters (a, c,V, D) and tolerance factor (t) for (La,Co) co-doped $BiFeO_3$

sample	Crystallite size D(nm)	t	Lattice parameters	Volume $V = \frac{\sqrt{3}}{2}a^2c$	
			a=b($\dot{A}$)	c($\dot{A}$)	
X=0 (BFO)	47[17]	0.95[7]	5.802[7]	13.87[7]	404.35
X=0.1	26.27042	0.889	5.627	13.85066	379.8
X=0.15	21.01448	0.888	5.543	13.54358	360.374

From Table 1, it is observed that the lattice parameters decreased as concentration of doping increase. It is also observed that the crystallite size as calculated from Debye- Scherer formula and volume of the unit cell decreased with increasing (La, Co) co-substituted BFO.

The pure $BiFeO_3$ (BFO) is well described by the rhombohedra structure with R3c space group [15,16]. The analysis has shown that as the concentration of the Ho doped in the place of Bi at A-site and Co doped in the place of Fe at the B-site in BFO, all the samples have changed from rhombohedrastructure to orthorhombic.

To confirm the distorted perovskite structure, Gold- schmidth tolerance factor(t) relation is used [16].

$$t = \frac{<R_A>+R_O}{\sqrt{2}(<R_B>+R_O)} \qquad (2)$$

Where$< R_A >$,$< R_B >$, and R_O, respectively are the average ionic radii of A-site, B-site and Oxygen. The calculated tolerance factor for x=0.10 to x=0.15 are shown in Table 1, indicating the crystal deviation from cubic perovskite structure (t=1) to orthorhombic (t=0.889 -0.88).This slight change in the crystal structure may lead to changed electric and magnetic properties [18].

3.2. FTIR Analysis

The room temperature FTIR spectra for all samples are shown in figure 2. The strong absorption peaks near 558 cm^{-1} and another near 432 cm^{-1} are assigned to O-Fe–O stretching and bending vibration, respectively, being characteristics of the octahedral FeO_6 group, which indicate the formation of $BiFeO_3$ perovskite structuretype[18-20].

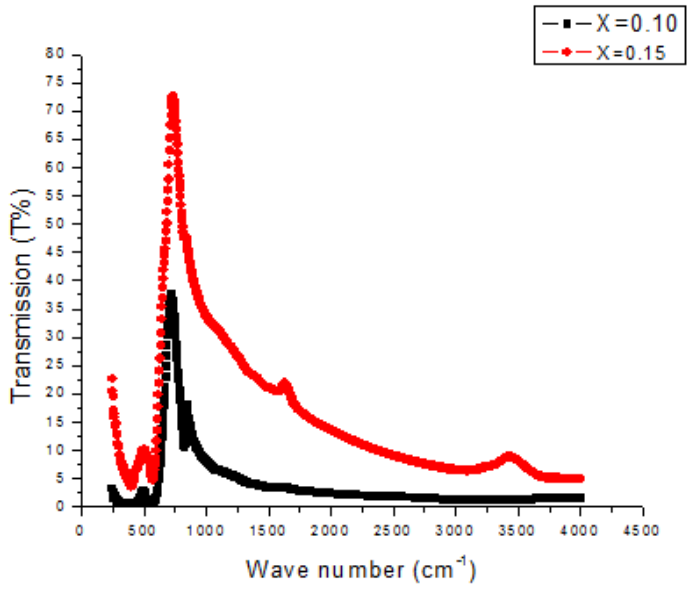

Fig.2, FTIR spectra of (La,Co) co-doped $BiFeO_3$

3.3. Microstructure Analysis

Figures 3a & b show the scanning electron micrographs (SEM) images of $Bi_{1-x}La_xFe_{0.85}Co_{0.15}O_3$ (x=0.10, 0.15) ceramics. From the micrographs, it is noticed that the morphology of the samples dense with non-uniform grains. The average grain size decreases with increasing of the co-doping contents. The reduction of the grain size with the co-doping is attributed to the incorporation of ions with smaller ionic radii of La^{3+} at Bi^{3+} -site and Co^{2+}at Fe^{3+} of BFO ceramics[21, 22].

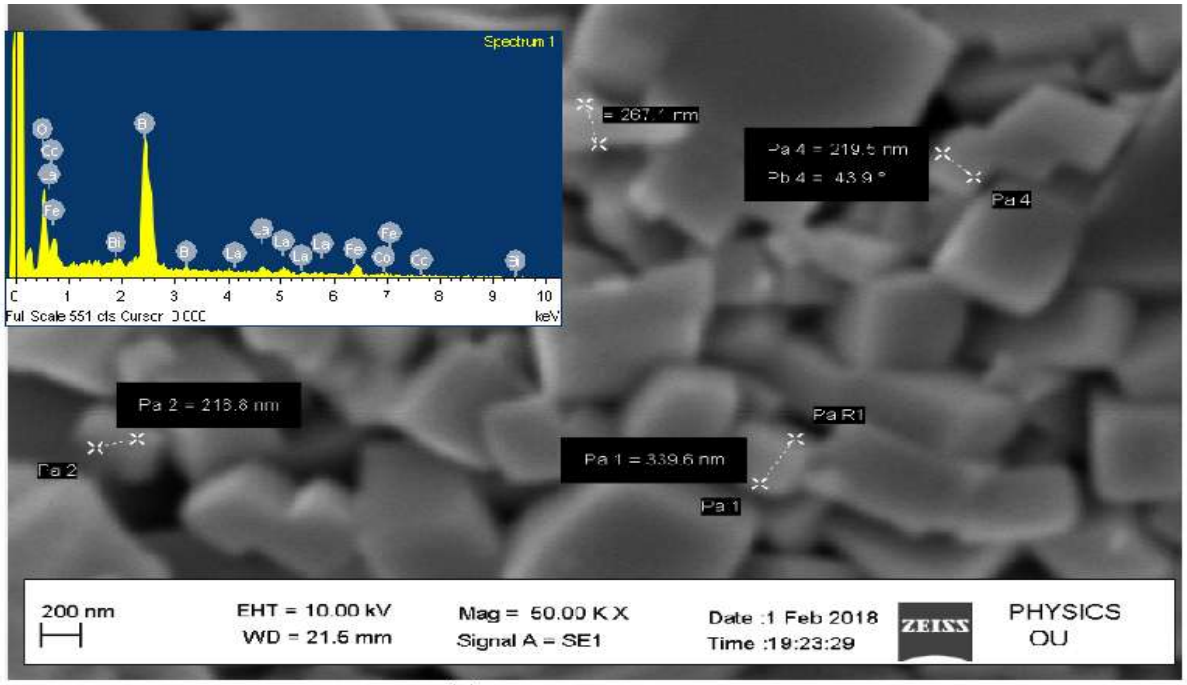

(a)

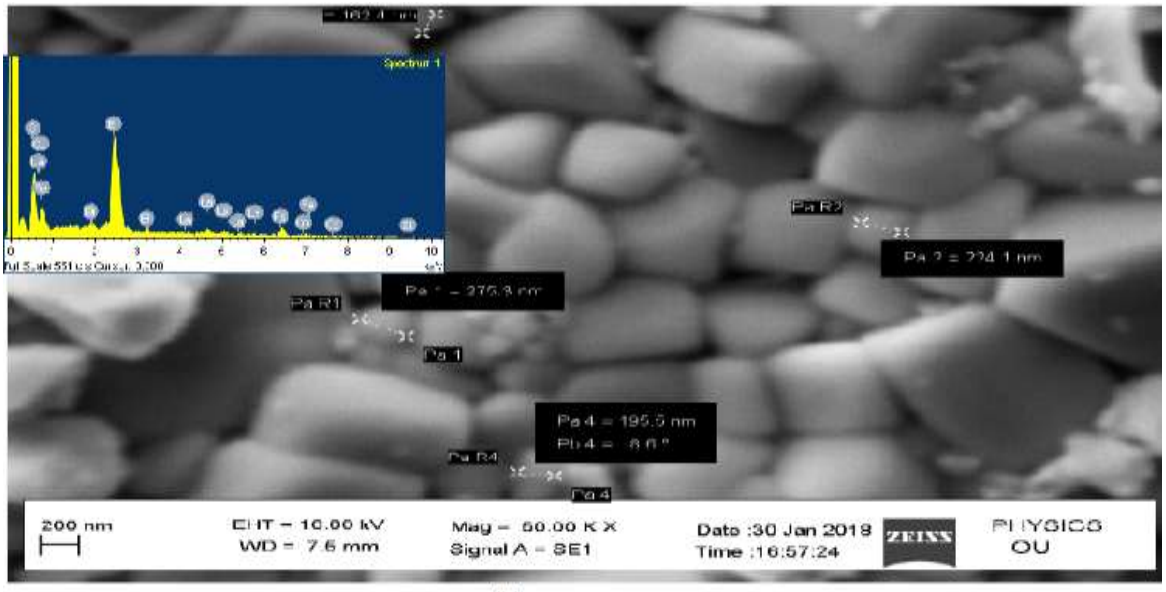

(b)

Fig.3. SEM and EDX (insert) images for (a) x=0.1 (b) x=0.15

In figure 3a&b the EDX spectrum (insert) of the ceramics confirmed the presence of the expected amount of Bi, La, Fe, Co and O as per the stoichiometry ratios.

3.4. Electric Modulus Studies

The frequency dependence of the imaginary part of the electric modulus (M") is used to provide information relating to charge transport process such as mechanism of electrical transport, conductivity relaxation and ionic dynamics [23].

Figures 4 a&b show the variation of imaginary part of electric modulus with the frequency of the applied field irrespective of the temperatures $(300^oC, 350^oC, 400^oC, 450^o, 500^oC)$ for the samples.

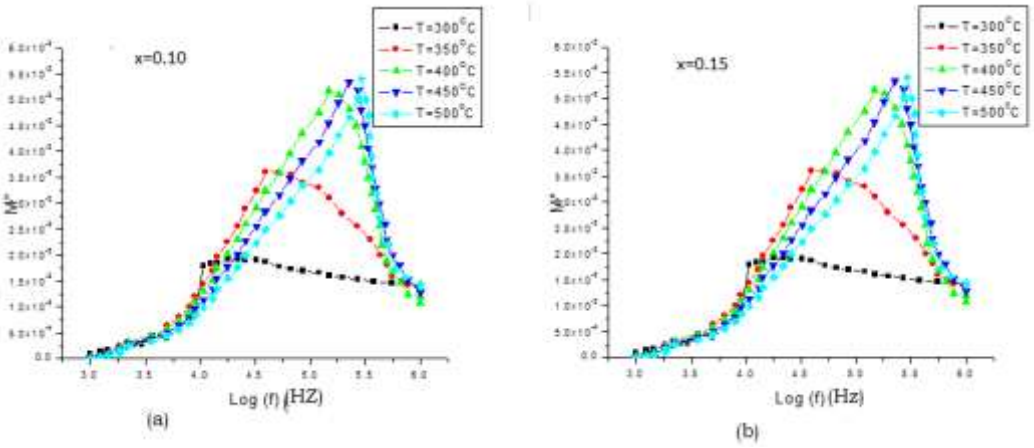

Figure 4 Variation of M" with frequency for a) x=0.10 b)x=0.15

From the figures 4, the maximum value ($M"max$) for each sample shifts towards the higher frequency side on increasing temperature which is related to the motions of the mobile ions over a long distance [24]. The frequency range where the peaks occur is the indication of a transition from long range to short range mobility of charge and the asymmetric peak broadening indicates a spread of relaxation times (τ) having different values with the respect to peak maximum whose positions are frequency and temperature dependent, and hence the relaxation of non-Debye type[25].

The spectra obtained from the results confirmed that there is hopping of carriers from one lattice site to the neighboring sit which contribute for electrical conduction of the material [20,26].

The activation energy for each concentration of the co-dopants can be calculated from the slope of the curve in $Log\ (\tau)$ versus 1000/Tas shown in figure 5. The results are summarized in Table .

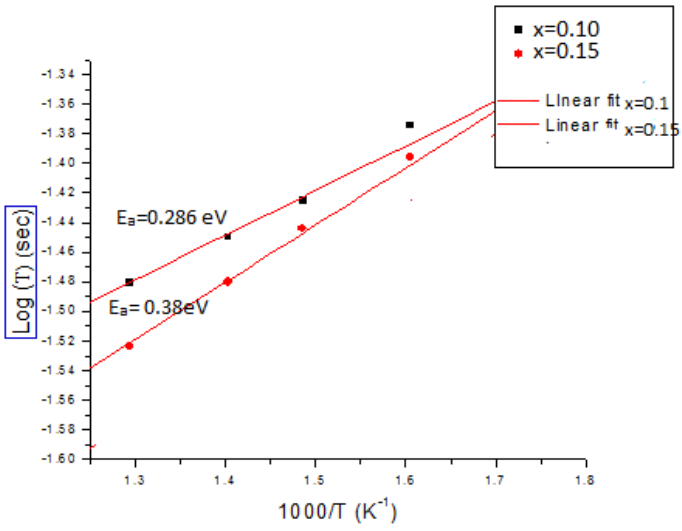

Figure 5 Variation of $Log\ (\tau)$ with 1000/T for $Bi_{1-x}La_xFe_{0.85}Co_{0.15}O_3$ (x=0.10, 0.15)

The variation of Log (τ) with the inverse of absolute temperature (Figure 5) for $Bi_{1-x}La_xFe_{0.85}Co_{0.15}O_3$ ceramics is derived from the impedance data plot in figure 4. using the Arrhenius relation[27]

$$\tau = \tau_o \exp(\frac{E_a}{k_B T}) \quad (3)$$

τ_o is the pre-exponential factor, Ea is activation energy in eV, k_B is the Boltzmann constant and T is the absolute temperature.

From the result obtained the value of relaxation time decrease with increasing absolute temperature for particular La and Co co-doped BFO sample. The results have also shown that the value of activation energy increase with increasing of the co-dopants concentration which is a typical behavior of the insulating nature of the grains in the ceramics, which is due to the suppression of oxygen vacancies. In this present work, the oxygen vacancies obtained may be due to the volatility of bismuth ion during final sintering at a temperature of 850^oC and may also be due Fe ion valance fluctuation when Co^{2+}substituted Fe^{3+}in BFO ceramic, changing $Fe^{3+}$to $Fe^{4+}$for charge compensation. This can be expressed as per Kroger-Vinknotation[28].

$$O_o^x = V_o^{''} + \frac{1}{2}O_2 + e" \quad (4)$$

O_o^x is the loss of lattice oxygen, $V_o^{''}$ is the presence of oxygen ion vacancy and e'' is the electron released or captured by Bi-site or Fe-site.

Table2 Variation of activation energy with La and Co co-doped BFO for different temperature

sample	Temperature (^oC)	Relaxation time, $\tau(\sim 10^{-6}sec)$	Activation energy (eV)
X=0.1	300	41.88	0.286
	350	27.04	
	400	9.163	
	450	4.7	
	500	2.41	
X=0.15	300	41.89	0.38
	350	21.48	
	400	5.92	
	450	1.39	
	500	0.76	

3.5. Ferroelectric Studies

Figure 6 shows the room temperature P-E hysteresis loop for $Bi_{1-x}La_xFe_{0.85}Co_{0.15}O_3$ (x=0.1, 0.15) ceramics. For the prepared samples the values of spontaneous polarization (Ps), remnant polarization (Pr) and coercive field (Ec) are summarized in Table 3.

Table 3 Measurement of electrical parameters from P-E hysteresis loops

Sample	Ps $(\mu C/cm^2)$	Es (kV/cm)	Pr$(\mu C/cm^2)$	Ec(kV/cm)
X=0.10	4.77	1.51	4.51, -4.46	1.07, -1.11
X=0.15	4.86	1.76	4.81 , --4.75	1.77 , -2.06

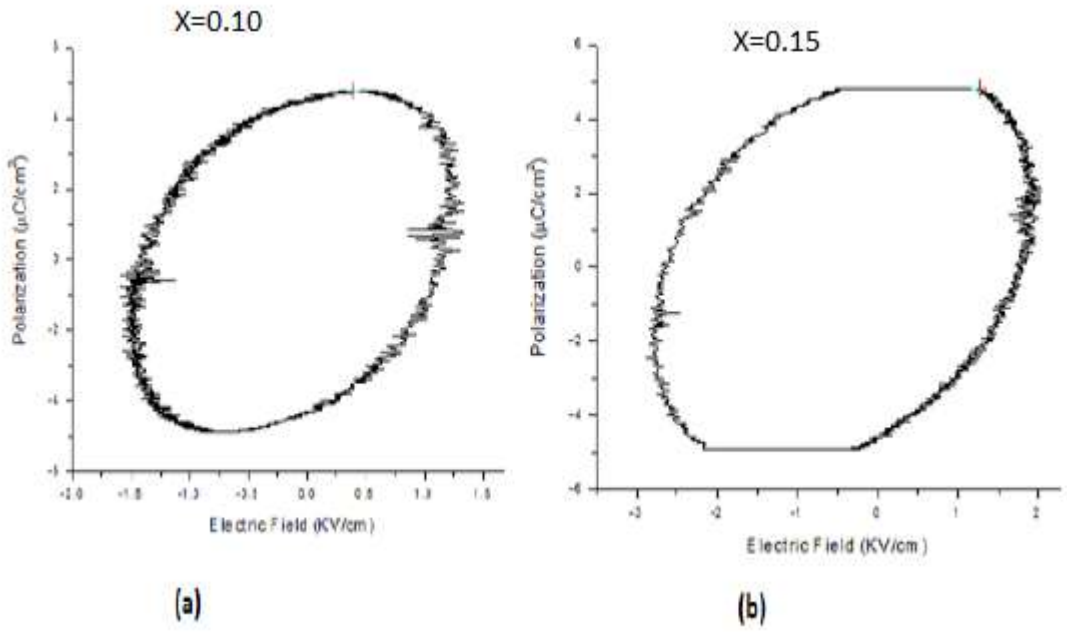

Figure 6 P-E hysteresis loops for $Bi_{1-x}La_xFe_{0.85}Co_{0.15}O_3$ (x=0.10, 0.15) ceramics

From figures, the shape of the curves obtained look like elliptical type with the sample x=0.15 is more saturated than that for x=0.10. The polarization level increase with the increasing of co-doping concentration. This increment may be due to The increased values may be attributed to maximum dielectric observed in the samples, because the co-doped led to improve the oxygen ion stability in lattice site of the ceramics and hence improve the fatigue resistance [25].

For both the samples the curves show slightly ferroelectric behavior, but not perfect ferroelectric which arise from the lossy nature of the material.

3.6. Magnetic Studies

Figure 7 shows the M-H loops for $Bi_{1-x}La_xFe_{0.85}Co_{0.15}O_3$ (x=0.10, 0.15) ceramics measured at room temperature. These loops were recorded by vibrating sample magnetometer"VSM Lakeshore-74071". The scanning range was set between 0 and10000 G(1T). The prepared samples show magnetic hysteresis loops representing ferromagnetic behavior. From the results obtained, the magnetic parameters such as saturated magnetization is increased from 13.24 emu/g for x=0.10 to 39.59 emu/g for x=0.15, the remnant magnetization (2Mr) is 6.158 emu/g for x=0.10 and 20.46 emu/g for x=0.15. The coercive field decreased from 774 G to 498 G when x increased from 0.10 to 0.15.

La and Co co-substitution of BFO play significant role in improving the magnetization of the ceramics. The improved in magnetic properties is due to the substitution of smaller ionic radius of La^{3+} ions at Bi^{3+} site in BFO resulting in decreasing the average ionic size of Bi-site which in turn decrease the tolerance factor (Table 1) and then increased in octahedral tilt of FeO_6 by changing in Fe-O-Fe bond angle and Fe-O bond length. The co-substitution resulted in the increase of the canting angle that suppressed anti-ferromagnetic ordering of the sub lattice, which is in agreement with the results obtained by Ahmad,S. et al.[5].

The co-doping of La and Co also leads to modification in spiral modulated spin structure resulting in ferromagnetic behavior in contrast to G-type anti-ferromagnetic of the present compound, which is in agreement with the result found by A. K. Jena and J. Mohanty [7].

The derived magnetic parameters from the hysteresis loops such as saturation magnetization (Ms), remnant magnetization (2Mr) and coercive field (2Hc) of co doped samples were summarized in Table 4.

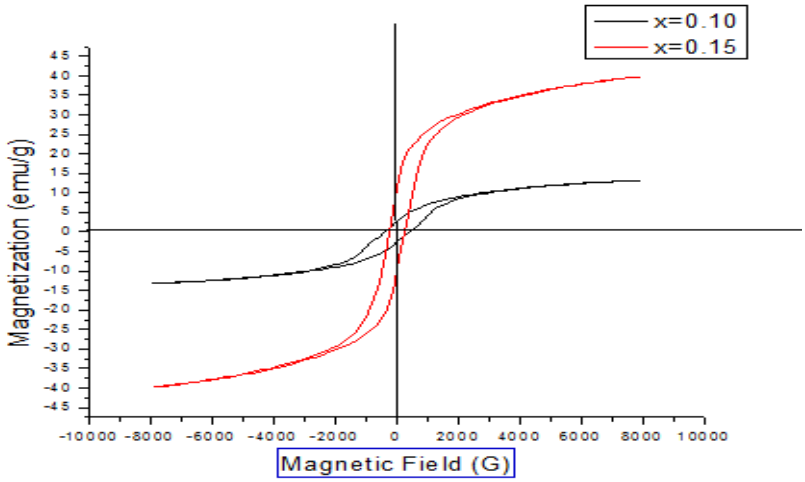

Figure 7 M-H hysteresis loop for $Bi_{1-x}La_xFe_{0.85}Co_{0.15}O_3$ (x=0.10, 0.15) ceramics

Table 4: Magnetic parameters extracted from M-H curves measured at room temperature for La and Co co-doped $BiFeO_3$

Sample	Saturation magnetization Ms(emu/g)	Hs (G)	Remnant magnetization 2Mr (emu/g)	Coercive Field ,2Hc (G)
BFO	0.070*[13]		0.0028*[13]	
X=0.1	13.24	7906.83	6.158	774
X=0.15	39.59	7906.10	20.46	498

Conclusion

The aim of this paper was to improve the magneto-electric property of $BiFeO_3$ by La^{3+} and Co^{2+} co-doping ions using sol-gel technique. From the results obtained, the XRD spectra and SEM micrographs confirmed that the crystal size decrease with increasing the co-doping contents, which is due to the incorporation of the smaller ionic radii of co-substitution ions. In the impedance measurement, the obtained activation energy increase with increasing the co-doping contents and decrease with increase of frequency which is attributed to size effect. The results have also shown us the ferroelectric properties are enhanced with co-substitution due to the suppressed oxygen vacancies which may arose from the volatility of the bismuth at elevated temperature. The room temperature magnetic measurement by VSM showed that the enhanced magnetic properties with the increasing the co-doping contents. The improved in magnetization is attributed to the suppression of spin spiral cycloid of G-type anti-ferromagnetic structure of BFO, as the result of the reduction of grain size (size effect). The significantly enhanced in both ferroelectric and magnetic properties (Magneto-electric) of the single material has potential application from technological point of view.

Acknowledgement

This work was financially supported by Wollega University (Ethiopia). Osmania University (India) supported us in permitting the laboratory room, especially, In-organic chemistry wet lab. The physic department helped us in permitting to use furnace, impedance analyzer. XRD, SEM, EDX, FTIR. University of Hyderabad also helped us to analyze the magnetic properties of our samples

References

1. MadboulyA. M., Effect of Gamma Radiation on Electrical Properties of $Bi_{1-x}Ca_xFeO_3$ Multiferroic, International Journal of Science and Research (IJSR), 2015, Volume 4 Issue 4, pp.210-217
2. Kuang, D., et al. (2016). Structural, optical and magnetic studies of (Y, Co) co-substituted $BiFeO_3$ thin films, J. Alloy Compd. 671, pp.192-199.

3. Mao W., Chen W., Wang X. et al., Influence of Eu and Sr co-substitution on multiferroic properties of $BiFeO_3$, Ceram. Int., 2016, 42 (11), pp. 12838-12842.
4. Tokura, Y., Seki, S., and Nagaosa, N. (2014). Multi-ferroics of spin origin, Rep. Prog. Phys.77(7), 076501
5. Ahmad S.,Muhammad, A. K.,MansoorS. et al., The impact of Yb and Co on structural, magnetic, electrical and Photo- catalytic behavior of nanocrystalline multiferroic $BiFeO_3$ particles, Ceramics International 43 pp.16880–16887, 2017.
6. Chakrabarti K., Das K., SarkarB., and De S. K., Magnetic and dielectric properties of Eu- doped $BiFeO_3$ nanoparticles by acetic acid-assisted sol-gel method, J. Appl., Phys. 2011, 110, 103905.
7. Jena A.K. and MohantyJ., Enhancing ferromagnetic properties in bismuth ferriteswith non‐magnetic Y and Sc co‐doping,Journal of Materials Science, Materials in Electronics, 2017.
8. Pandu R. , $CrFe_2O_4$–$BiFeO_3$perovskitemultiferroicnano-composites, a review, Mater. Sci. Res. India, 2014, 11, pp.128–145
9. Pandit P., SatapathyS. P., Gupta K. and Sathe V.G., Effect of coalesce doping of Nd and La on structure, dielectric, and magnetic properties of $BiFeO_3$, J. Appl. Phys., 2009, 106.
10. Rao T. D., Ranjith R. and Asthana S., Enhanced magnetization and improved insulating character in Eu substituted $BiFeO_3$, J. Appl. Phys.,2014, 115, 124110.
11. Zhao S. and Yun Q., Enhanced ferromagnetism of Ho, Mn co-doped $BiFeO_3$ nanoparticles, Integr. Ferroelectric, 2013, 141, pp. 18–23
12. Tadic M., Jagodic M.,Kralj S.,Hanzel D., Magnetic properties of novel superparamagnetic iron oxide nanoclusters and their peculiarity under annealing treatment, Appl. Surf. Sci., 2014, 322, 255–264
13. Mao W.,Wang X., Han Y., Li X.., Li Y., Wang Y., MaY., Feng X., Yang T., Yang J., Huang W., Effect of Ln (Ln = La, Pr) and Co co-doped on the magnetic and ferroelectric properties of $BiFeO_3$ nanoparticles, J. Alloy, Compd., 2014,. 584, pp.520–523.
14. Ye W., TanG., DongG.,Ren H., XiaA., Improved multiferroic properties in(Ho, Mn) co- doped $BiFeO_3$ thin films prepared by chemical solution deposition, Ceramics International, 2015, 41, pp.4668–4674.
15. Yan X., Liu W.,Tan G., Ren H., Structural, electric and magnetic properties of Dy and Mnco-doped $BiFeO_3$ thin film, Ceram. Int., 2015, 41, pp. 3202–3207.
16. Klug H.P. & Alexander L.E., X-ray Diffraction Procedures, Wiley, New York, 1974.
17. SinhaA.K., BhushanB., RoutD., Sharma R. K. et al.,Structural and magnetic properties of Cr doped $BiFeO_3$multiferroic nanoparticles, AIP Conference Proceedings, 2017, 1832, 050088.
18. Arya G., KumarA., Ram M. and NegiN. S. , Structural, dielectric, ferroelectric and magnetic properties of Mn- doped $BiFeO_3$ nanoparticles synthesized by Sol-Gel Method. International Journal of Advances in Engineering & Technology, 2013, Vol. 5, Issue 2, pp. 245-252
19. Erdenee N., Enkhnaran U., Galsan S., and Pagvajavet A., Lanthanum-Based Perovskite-Type Oxides $La_{1-x}Ce_xBO_3$ (B=Mn and Co) as Catalysts: Synthesis and Characterization, Hindawi Journal of Nanomaterials, 2017, 8 pages.
20. KaurB.,Singh L., Reddy V. A., JeongD.-Y. et al., AC Impedance Spectroscopy, Conductivity and Optical Studies of Sr doped Bismuth Ferrite Nanocomposites.Int. J. Electrochem. Sci.,2016,11, pp4120 – 4135
21. Ray J., Biswal A.K., Acharya S., Ganesan V., Pradhan D.K., VishwakarmaP.N., Effect of co-substitution on the magnetic properties of $BiFeO_3$. J Magnetic Material, 2012, 324, pp4084–4089
22. Khan U., Influence of cobalt doping on structural and magnetic properties of $BiFeO_3$ nano-particles. Journal of Nano-particleResearch, 2015, 17:429.
23. Anwar, Z.M.,Khan M. A, Ali I., AsgharM. et al.(2014). Investigation of Dielectric Behavior of New Tb^{3+} Doped $BiFeO_3$nano crystals Synthesized Via Micro-Emuslion Route. Journal Research,.2014, Vol.10,No. 6, pp.265-273
24. Pattanayak S., parida B.N. and Das P.R.,Impedance Spectroscopy of Gd doped $BiFeO_3$Multiferroics. Appl. Phys A,2013, 112, pp. 387-395.
25. PattanayakS.,Parida B.N., Das P.R., Choudry R.N.P., Effect of Dysubstitution on structural, electrical and magnetic properties of multiferroic $BiFeO_3$ ceramics, Ceramics International, 2014, 40(6), 7983-7991.
26. Badapanda T.,Harichandan K. R., Nayak S. S.,Mishra A., Anwar S., Frequency and Temperature dependence behavior of impedance, Modulus and conductivity of $BaBi_4Ti_4O_{15}$Aurivillus Ceramics. Processing and Applicationof Ceramics, 2014, 8(3), pp.145-153.

27. Thakur S., Rai R., BdikinI. and Valente*c* A.M.,Impedance and Modulus Spectroscopy Characterization of Tb modified $Bi_{0.8}A_{0.1}Pb_{0.1}Fe_{0.9}Ti_{0.1}O_3$ Ceramics**.** Materials Research, 2016, 19(1): pp1-8.
28. Kroger F.A. and Vink H., J. Solid state Physics 3, Material Science, 1956, 41, 369.

*****